Quarterly Technical Report

Growth, Characterization and Device Development in Monocrystalline Diamond Films

Supported under Grant #N00014-93-I-0437
Office of the Chief of Naval Research
Report for the period 1/1/97–3/31/97

R. F. Davis, R. J. Nemanich* and Z. Sitar
P. Baumann, W. Liu, R. Schlesser, C. A. Wolden, and P. C. Yang
North Carolina State University
c/o Materials Science and Engineering Department
*Department of Physics
Box 7907
Raleigh, NC 27695

March 1997

REPORT DOCUMENTATION PAGE

Form Approved
OMB No. 0704-0188

1. AGENCY USE ONLY *(Leave blank)*	2. REPORT DATE	3. REPORT TYPE AND DATES COVERED
	March, 1997	Quarterly Technical 1/1/97-3/31/97

4. TITLE AND SUBTITLE

Growth, Characterization and Device Development in Monocrystalline Diamond Films

5. FUNDING NUMBERS

s400003srr14
1114SS
N00179
N66005
4B855

6. AUTHOR(S)

R. F. Davis, R. J. Nemanich, and Z. Sitar

7. PERFORMING ORGANIZATION NAME(S) AND ADDRESS(ES)

North Carolina State University
Hillsborough Street
Raleigh, NC 27695

8. PERFORMING ORGANIZATION REPORT NUMBER

N00014-93-I-0437

9. SPONSORING/MONITORING AGENCY NAMES(S) AND ADDRESS(ES)

Sponsoring: ONR, Code 312, 800 N. Quincy, Arlington, VA 22217-5660
Monitoring: Admin. Contracting Officer, ONR, Regional Office Atlanta
101 Marietta Tower, Suite 2805
101 Marietta Street
Atlanta, GA 30323-0008

10. SPONSORING/MONITORING AGENCY REPORT NUMBER

11. SUPPLEMENTARY NOTES

12a. DISTRIBUTION/AVAILABILITY STATEMENT

Approved for Public Release; Distribution Unlimited

12b. DISTRIBUTION CODE

13. ABSTRACT ***(Maximum 200 words)***

Real time *in-situ* laser reflectometry was used to investigate changes in surface morphology observed during the nucleation of oriented diamond on Ni in a hot filament chemical vapor deposition reactor. Characteristic features observed in the intensities of reflected and scattered light were interpreted by comparison with scanning electron micrographs of the diamond seeded substrates quenched at sequential stages of the process. Based on this analysis, a process was developed in which the scattered light signal was used as a steering parameter. Oriented nucleation and growth of diamond on Ni was repeatedly achieved using this process. The evolution from diamond surfaces to metal-diamond interfaces has also been studied. The electron affinity and the Schottky barrier height of Zr and Cu films a few Å thick and deposited in UHV onto IIb diamond substrates cleaned by different anneals and plasma treatments in UHV were correlated. The initial surfaces were terminated with oxygen or free of chemisorbed species. UPS allowed the determination of a positive electron affinity or an NEA before and after metal deposition. The Schottky barrier height changed little in the presence or absence of chemisorbed species at the interface. An NEA was observed for Zr on diamond independent of the surface termination. For Cu, the surface cleaning prior to metal deposition had a more significant effect. The Schottky barrier height changed strongly depending on the chemical species at the interface. An NEA was only detected for Cu on clean diamond surfaces. The differences between Zr on one hand and Cu on the other are correlated with differences in interface chemistry and structure.

14. SUBJECT TERMS

diamond, chemical vapor deposition, nickel solution, laser reflectometry, surface morphology, oriented nucleation and growth, electron affinity, Schottky barrier height, zirconium, copper, interface chemistry, interface structure

15. NUMBER OF PAGES

18

16. PRICE CODE

17. SECURITY CLASSIFICATION OF REPORT	18. SECURITY CLASSIFICATION OF THIS PAGE	19. SECURITY CLASSIFICATION OF ABSTRACT	20. LIMITATION OF ABSTRACT
UNCLAS	UNCLAS	UNCLAS	SAR

Table of Contents

I.	Introduction	1
II.	Control of Diamond Heteroepitaxy on Nickel by Optical Reflectance *P. C. Yang, R. Schlesser, C. A. Wolden, W. Liu, R. F. Davis and Z. Sitar*	2
III.	Comparison of Electron Affinity and Schottky Barrier Height of Zirconium and Copper-Diamond Interfaces *P. K. Baumann and R. J. Nemanich*	8
IV.	Distribution List	18

I. Introduction

Diamond as a semiconductor in high-frequency, high-power transistors has unique advantages and disadvantages. Two advantages of diamond over other semiconductors used for these devices are its high thermal conductivity and high electric-field breakdown. The high thermal conductivity allows for higher power dissipation over similar devices made in Si or GaAs, and the higher electric field breakdown makes possible the production of substantially higher power, higher frequency devices than can be made with other commonly-used semiconductors.

In general, the use of bulk crystals severely limits the potential semiconductor applications of diamond. Among several problems typical for this approach are the difficulty of doping the bulk crystals, device integration problems, high cost and low area of such substrates. In principal, these problems can be alleviated via the availability of chemically vapor deposited (CVD) diamond films. Recent studies have shown that CVD diamond films have thermally activated conductivity with activation energies similar to crystalline diamonds with comparable doping levels. Acceptor doping via the gas phase is also possible during activated CVD growth by the addition of diborane to the primary gas stream.

The recently developed activated CVD methods have made feasible the growth of polycrystalline diamond thin films on many non-diamond substrates and the growth of single crystal thin films on diamond substrates. More specifically, single crystal epitaxial films have been grown on the {100} faces of natural and high pressure/high temperature synthetic crystals. Crystallographic perfection of these homoepitaxial films is comparable to that of natural diamond crystals. However, routes to the achievement of rapid nucleation on foreign substrates and heteroepitaxy on one or more of these substrates has proven more difficult to achieve. This area of study has been a principal focus of the research of this contract.

At present, the feasibility of diamond electronics has been demonstrated with several simple experimental devices, while the development of a true diamond-based semiconductor materials technology has several barriers which a host of investigators are struggling to surmount. It is in this latter regime of investigation that the research described in this report has and continues to address.

In this reporting period, (1) real time *in situ* laser reflectometry was used to investigate changes in surface morphology observed during the nucleation of oriented diamond on Ni in a hot filament chemical vapor deposition reactor and (2) electron affinity and Schottky barrier height of thin Cu and Zr films on diamond (100) substrates were correlated by means of UV photoemission spectroscopy (UPS) measurements. The following sections are self-contained in that they present an introduction, the experimental procedures, results and discussion, summary and indications of future research for the given research thrust.

II. Control of Diamond Heteroepitaxy on Nickel by Optical Reflectance

1. Introduction

The growth of heteroepitaxial films represents an important step toward the attainment of large-area, device-quality diamond. The high surface energy of diamond and interfacial stress between diamond films and non-diamond substrates are believed to be primary obstacles to the formation of oriented, two-dimensional diamond nuclei. Nickel is one of a few materials that has a small lattice mismatch with diamond (a=3.52Å for Ni vs. a=3.56Å for diamond). It has been known for decades that Ni is an effective solvent-catalyst for diamond crystallization under high pressure and high temperature (HPHT) conditions [1]. Some success has been attained using Ni as a substrate for diamond growth by low pressure chemical vapor deposition. Sato [2] reported that both (111) and (100) oriented diamond nuclei could be grown on Ni substrates, but the overall percentage of oriented nuclei was rather low. We have observed that under certain conditions, oriented diamond nuclei precipitate from a supersaturated Ni-C-H solution [3,4]. A similar phenomenon has been observed for the heteroepitaxial growth of diamond on (111) platinum by Kobashi and Tachibana [5]. Roy [6] also reported on precipitation of diamond particles from different mixtures of diamond and metal powders. Despite these successes, the mechanism by which oriented nuclei are formed is not understood. Also, the high catalytic activity of Ni for hydrocarbon decomposition and high solubility of carbon in Ni often lead to either graphite deposition or no growth if the process is not properly controlled. In order to overcome these difficulties, we developed a multi-step seeding and growth process to obtain oriented diamond on nickel [3,4]. The process is very sensitive to the substrate temperature and requires accurate timing of both the nucleation and growth steps. Accurate process control is requisite to initiate diamond growth and to suppress the deposition of graphitic products. It has been observed that the surface morphology changes dramatically during the nucleation process and that *in situ* monitoring of the surface structure can provide valuable feedback for process control.

This section reports on the use of optical reflectometry to monitor changes in surface morphology in real time throughout the diamond seeding, annealing and growth steps. Reflected and scattered light signals were correlated with surface structures by comparison with scanning electron micrographs of samples that were quenched at different stages of the nucleation process. Based on these studies, a process control procedure was developed where experimental parameters were adjusted as a function of the scattered light signal. This control has significantly improved both the reproducibility and overall quality of the oriented diamond films on Ni substrates.

B. Experimental Procedure

The growth experiments were performed in a hot filament CVD diamond growth system that was described previously [3,4]. The chamber was modified to allow *in situ* optical measurements of reflective and scattering properties of the sample surface. Figure 1 shows the set-up of the optical monitoring system. A He-Ne laser (λ=633nm) illuminated the sample under normal incidence. A prism was used as a semi-transparent beam splitter which directed the reflected beam from the sample to a photodiode (detector 1). Light scattered from the sample surface was detected by a second photodiode positioned at an angle of 5° from the surface normal. The field of view for detector 2 was defined by a pair of apertures. In order to discriminate between the probe beam and the intense light of the filament used for dissociation of H_2, each detector was equipped with an optical interference filter. Furthermore, the incident laser beam was mechanically chopped (υ= 500 Hz). The relatively strong reflected signal was processed by an AC to DC RMS converter, which suppressed the constant filament light contribution. A phase-sensitive lock-in amplifier was used to detect the weaker scattering signal. The substrate temperature was measured by a type C thermocouple imbedded ~100μm beneath the substrate surface. All optical and temperature signals were recorded simultaneously by a Macintosh-based data acquisition system.

The experimental procedure used to generate oriented diamond nuclei consisted of three steps. First, a polished nickel substrate was seeded with a loosely applied layer of submicron diamond powder. Subsequently, the substrate was heated by the hot filament in a hydrogen

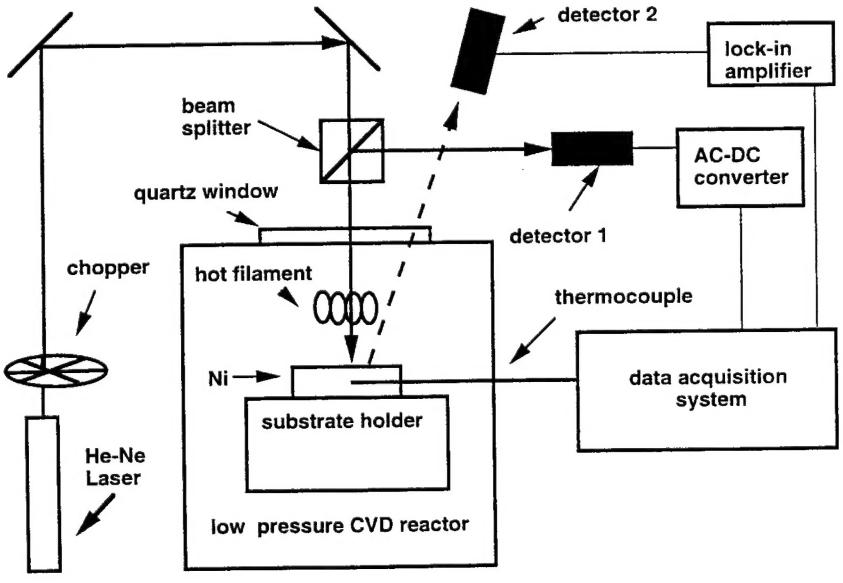

Figure 1. Schematic of the hot-filament reactor equipped with optical diagnostics that used for heteroepitaxial nucleation and growth of diamond on nickel.

environment to a relatively high temperature (~1100°C) for a short annealing time (3-10 mins) to produce a C-saturated surface. Finally, the temperature was lowered to ~900°C and methane was introduced to initiate gas phase growth of diamond.

C. Results and Discussion

Typical changes in the intensities of reflected light, scattered light, and substrate temperature during the high-temperature anneal are shown in Fig. 2. Initially, the reflected light intensity was weak due to considerable scattering losses on the diamond seeds. The substrate temperature was rapidly increased to above 1000°C, eventually saturating at 1050°C. Simultaneously, a transient peak was observed in the scattered light intensity accompanied by a rapid increase in the reflected light signal. At the high temperatures the reflected light reached a maximum, while the scattered light signal dropped back to its initial value. The typical changes in the optical signals (i.e., the rapid increase in reflectivity, accompanied by a transient peak in scattered intensity) were found to be reproducible from run to run and, therefore, provided a powerful tool for monitoring and controlling the pregrowth stage of the growth process.

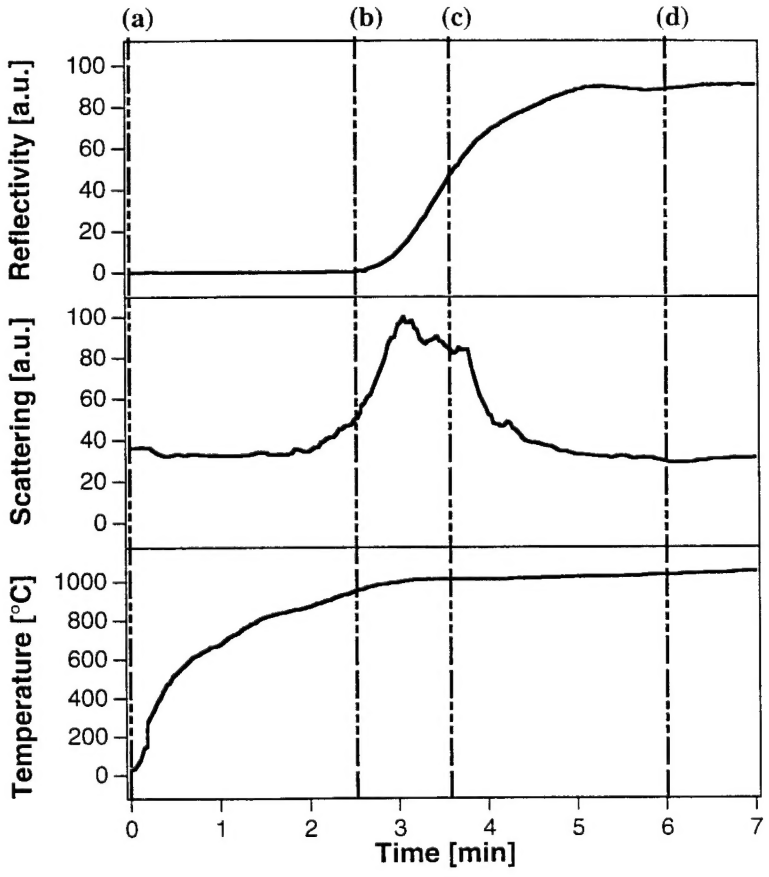

Figure 2. Typical changes in the intensities of reflected light, scattered light, and substrate temperature during the nucleation process.

In order to correlate the observed optical signals with surface features, samples were quenched at four stages (labeled a,b,c,d) of the process as indicated in Fig. 2. The quenched samples were analyzed by scanning electron microscopy and results are shown in Fig. 3. In the beginning (a), the Ni substrate was covered by a layer of diamond seeds produced by the seeding step. At time (b), as the reflected light intensity began to increase, the layer of diamond seeds was no longer continuous or uniform in size. A large fraction of the diamond seeds were either dissolved into the substrate or were etched away by atomic hydrogen. At the time (c), when the scattered light was most intense, the population of the diamond seeds was greatly

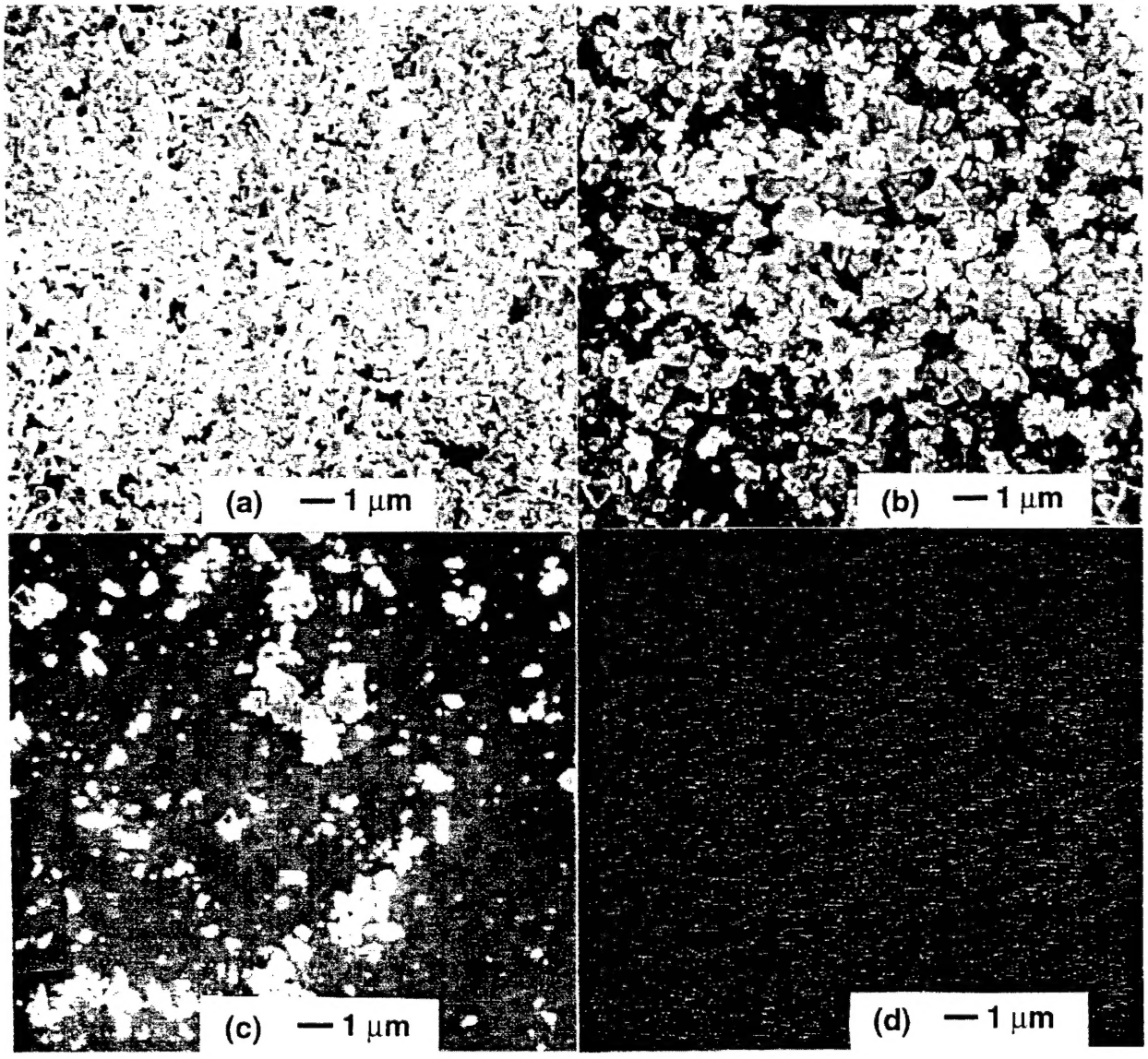

Figure 3. Surface morphologies of samples quenched at four different stages of the nucleation process, as indicated in Fig. 2.

reduced and the size had become more uniform ranging from 100 to 200 nm. At time (d) the reflected light had saturated at a maximum intensity and the scattered light intensity decreased. At this point all the diamond seeds had disappeared from the surface and upon quenching an ordered crystalline surface morphology was obtained (Fig. 3d).

Based on its sensitivity to changes in surface morphology, the scattered light signal was chosen as the indication of the time to change the experimental conditions from the pretreatment stage to the normal growth stage. In order to achieve oriented diamond nucleation, the diamond seeds must be fully reacted with the nickel substrate. This was indicated by a rapid decrease in the scattered light intensity after the peak (Fig. 2). Because carbon would further diffuse into the substrate, maintaining a high temperature for a long time would reduce the carbon rich environment at the surface and subsequently lower the nucleation density. Therefore, following the drop in the scattered light signal the substrate temperature was lowered from 1050°C to 900°C and 0.5% CH_4 was added to the H_2 gas flow. The change in scattered light signal during a complete process is shown in Fig. 4a. The steady increase in scattered light signal after lowering of the substrate temperature was attributed to the nucleation and growth of diamond. After 5 hours of growth at 900°C, oriented diamond was obtained as shown in Figure 4b.

D. Conclusions

Optical reflectometry has been demonstrated to be a technique sensitive to morphology changes associated with the seeding and annealing process of diamond on Ni substrates. It was found that a transient increase in the scattered light intensity can be used as a control parameter. Use of scattered light as a process control resulted in reproducible production of oriented diamond on nickel.

E. References

1. R. H. Wentorf, Jr., Adv. Chem. Phys. **9**, 365 (1965).
2. Y. Sato, H. Fujita, T. Ando, T. Tanaka, and M. Kamo, Phil. Transactions of the Royal Society of London **A342**, 225 (1993).
3. P. C. Yang, W. Zhu, and J. T. Glass, J. Mater. Res. **8**, 1773 (1993).
4. P. C. Yang, W. Zhu, J. T. Glass, U.S. Patent No. 5 298 286 (1994).
5. T. Tachibana, Y. Yokota, K. Nishimura, K. Miyata, K. Kobashi, and Y. Shintani, Diamond and Rel. Mater. **5**, 197 (1996).
6. H. S. Dewan, D. Ravichandran, J. P. Cheng, W. R. Drawl, K. A. Cherian, and R. Roy, *Proc. of the Applied Diamond Conference*, 1995, Gaithersburg, MD, p. 387.

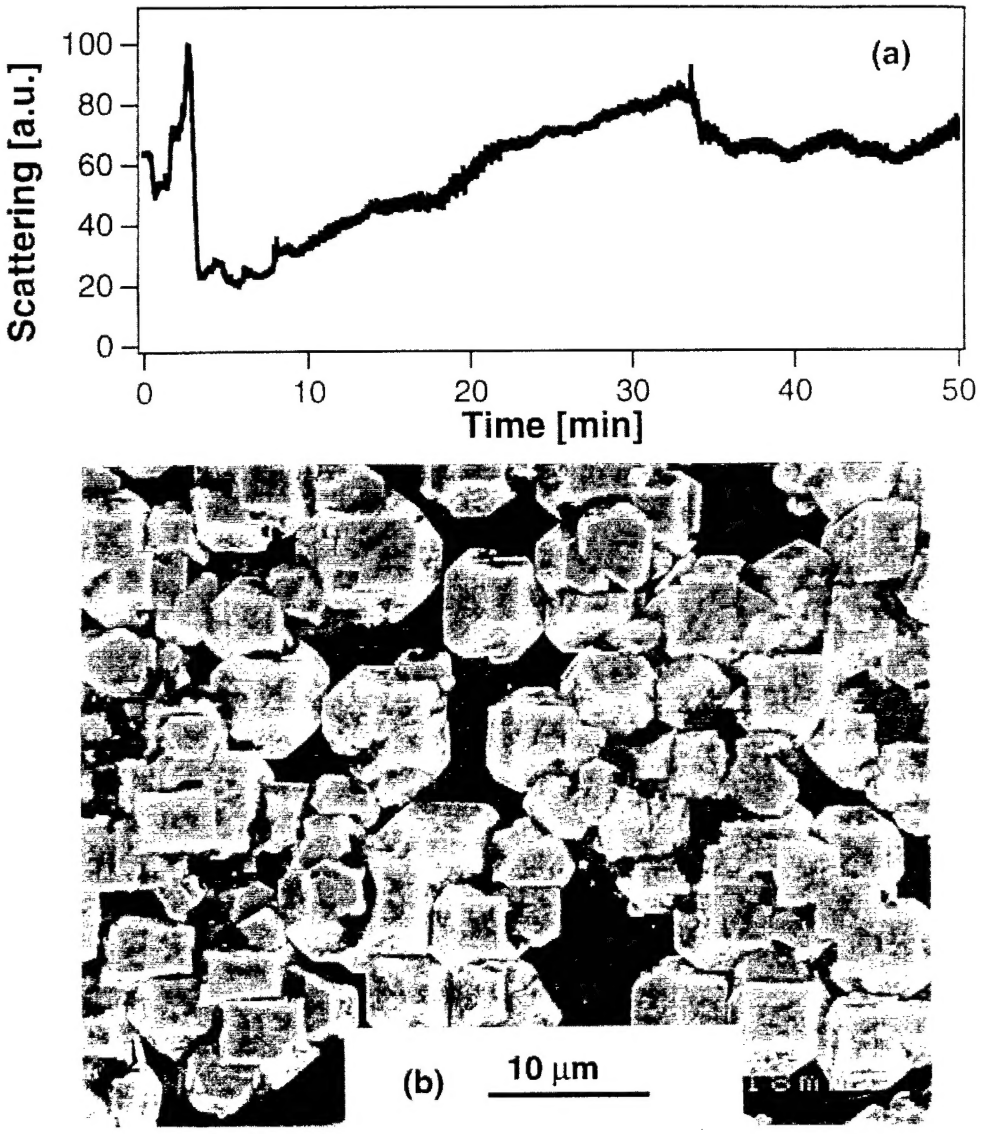

Figure 4. (a) Changes in the scattered light intensity throughout the annealing and growth process, and (b) SEM micrograph of resulting diamond film on Ni.

III. Comparison of Electron Affinity and Schottky Barrier Height of Zirconium and Copper-Diamond Interfaces

A. Introduction

Negative electron affinity (NEA) surfaces could enable the development of cold cathode devices. The electron affinity of a semiconductor corresponds to the energy difference between the vacuum level and the conduction band minimum. For most materials, the vacuum level lies above the conduction band minimum. This is called a positive electron affinity. As a wide bandgap semiconductor, diamond has the potential of exhibiting negative electron affinity surfaces since the conduction band minimum lies near the vacuum level. Electrons from the conduction band minimum then have sufficient energy to leave a NEA surface and be emitted into vacuum.

By employing different surface treatments such as plasma cleaning or annealing in ultra high vacuum (UHV), the position of the conduction band minimum can be shifted with respect to the vacuum level. This can induce a NEA or remove it [1-6]. Subsequent to pre-cleaning the diamond (100) samples with a wet chemical etch, the diamond surfaces are oxygen terminated. This chemisorbed oxygen layer forms a surface dipole. Such a surface exhibits a positive electron affinity. For the diamond (100) surface, an anneal to 900°C–1050°C or a H-plasma clean results in a NEA and a 2×1 reconstructed, oxygen free surface [3, 5, 6]. The different threshold temperatures are related to different wet chemical pre-treatments [3]. It was found that UHV annealing at 900°C was sufficient for samples pre-cleaned by an electrochemical etch. But a 1050°C anneal was required for a pre-clean employing chromic acid. It has been proposed that the diamond (100) surface exhibits a monohydride termination subsequent to a 900°C–1050°C anneal or a H-plasma exposure [3, 5, 6]. An H surface layer results in a dipole resulting in a NEA. However, for all these treatments a positive electron affinity and a 2×1 reconstruction are observed following a 1150°C anneal [6]. This surface is considered to be free of adsorbates. *Ab initio* calculations for the 2×1 reconstructed surface predict a NEA for a monohydride terminated surface and a positive electron affinity for an adsorbate free surface [5]. This is in agreement with the experimental results [5, 6].

It has been demonstrated that depositing a few Å of metals such as Ti, Ni Co, Cu and Zr can induce a NEA on diamond surfaces [3, 7-12]. The presence of a NEA or positive electron affinity has been correlated with different structures of the metal–diamond interface. Metal films deposited on adsorbate free surfaces have been found to exhibit lower Schottky barrier heights and lower electron affinities than for surfaces terminated by species such as hydrogen or oxygen. And for some metal–diamond structures the Schottky barrier heights have been low enough to induce a NEA.

Photoemission spectroscopy is a very sensitive technique to determine whether a surface exhibits a NEA or a positive electron affinity. Electrons are photoexcited from the valence band into states in the conduction band. These electrons can then quasi-thermalize down to the conduction band minimum. For NEA surfaces, these secondary electrons from the conduction band minimum can be emitted into vacuum and appear as a sharp peak at the low kinetic energy end of the photoemission spectra [13, 14]. In this study, diamond (100) surfaces have been cleaned by anneals to 1050°C or 500°C. Thin Zr or Cu films were deposited on these diamond substrates. The surface properties were analyzed before and after metal deposition.

B. Experimental Procedure

For this study, a UHV system was employed that consists of several interconnected chambers featuring capabilities for annealing, metal deposition, UPS, LEED and AES. Several natural type IIb single crystal semiconducting, boron-doped diamond (100) substrates ($3.0 \times 3.0 \times 0.25$ mm) were used. Typical resistivities of these samples were 10^4 Ω cm. To remove non-diamond carbon and metal contaminants, an electrochemical etch was employed. Details of this method have been previously described [15]. The wafers were blown dry with N_2, mounted on a Mo holder and transferred into the UHV system (base pressure ~1×10^{-10} Torr). Two different *in vacuo* cleaning processes were employed to study the effect of surface treatment on the characteristics of the metal–diamond interface. These processes consisted of an anneal to either 1150°C or 500°C both for 10 minutes. The pressure in the annealing chamber rose from 1×10^{-10} Torr to 7×10^{-9} Torr and 8×10^{-10} Torr during the anneals, respectively. After the heat treatment 2Å thick layers of Zr or Cu were deposited onto the diamond surface. The deposition was facilitated by an e-beam evaporator. The pressure in the chamber rose to 2×10^{-9} Torr during deposition. A quartz crystal monitor was employed to determine the thickness of the metal films. Following the annealing and the growth steps, UPS and AES were employed to characterize the surface properties.

The presence of Zr or Cu on the surface was confirmed by using AES. AFM images of the diamond wafers clearly showed arrays of linear groves parallel to each other with a depth of ~20 Å. This surface structure was a result of the commercial polishing procedure used to smoothen the surfaces. Subsequent to depositing 2Å of metal, no island structures were observed in AFM measurements. This is indicative of a uniform 2D layer for both Zr and Cu.

He I (21.21 eV) radiation from a discharge lamp was employed to facilitate the photoemission. The emitted electrons were measured using a 50 mm hemispherical analyzer with an energy resolution of 0.15 eV. The sample was biased by 1V with respect to the analyzer. This was necessary so the low energy electrons from NEA surfaces could be detected despite the workfunction of the analyzer. The sharp NEA peak appears at the low energy end of the photoemission spectrum and corresponds to the energy position of the conduction band

minimum E_C (Fig. 1). Emission from E_C is positioned at $E_V + E_G$ in the spectrum. E_V is the energy position of the valence band maximum and E_G the energy of the bandgap. In a corresponding manner, emission from E_V appears at $E_V + h\nu$ in the UPS spectra. This corresponds to the high kinetic energy cutoff of the spectra for semiconductors. The spectral width for NEA surfaces, or the distance between emission from the valence band maximum and the conduction band minimum is then given by $h\nu - E_G$. With the values for He I radiation $h\nu = 21.21$ eV and the bandgap of diamond $E_G = 5.47$ eV, the width of the spectrum is 15.7 eV. However, for a surface with a positive electron affinity, the low energy cutoff is determined by the vacuum level. Then the spectral width will be smaller than for a NEA. In fact, the width will be reduced by the value of the positive electron affinity of the surface.

Consider photoemission spectra of a thin metal film on a semiconductor. Spectra exhibiting features from both the metal and the semiconductor can be used to determine the Schottky barrier height Φ_B (Fig. 2). For this to be the case, the thickness of the metal layer needs to be equal to or less than the electron mean free path (≤ 5 Å). The Schottky barrier

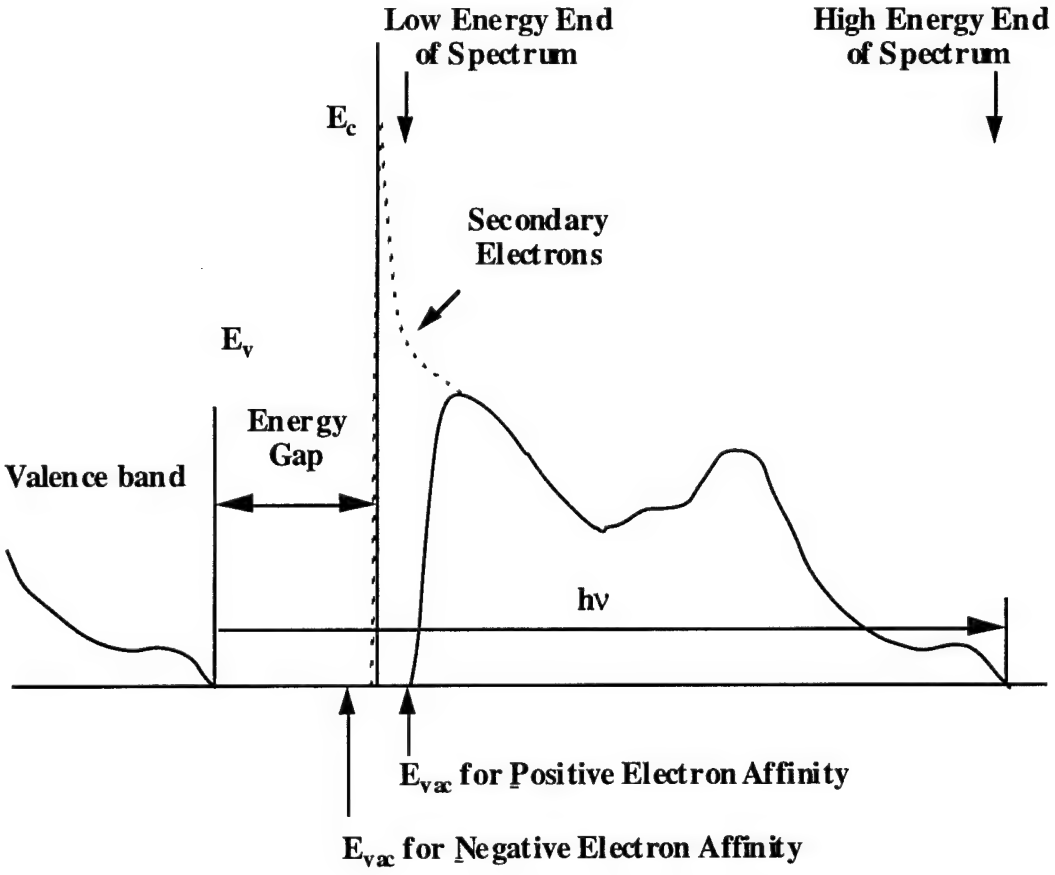

Figure 1. Schematic diagram of photoemission spectra for a negative electron affinity surface (dotted line) and a positive electron affinity surface (solid line).

height for a metal on a p-type semiconductors like diamond is defined by the difference between the position of the Fermi level of the metal, E_F and the valence band edge, E_V, of the semiconductor. It may, however, be difficult to detect the relatively weak onset of emission at E_V, even for metal layers thinner than the mean free path. This is due to the fact that emission from the metal Fermi level may overshadow this weak onset. Often times it is, therefore, necessary to use an independent method to determine the position of the valence band minimum. In particular, E_V can be referenced to some strong features in the diamond spectrum before metal deposition. Here, a peak positioned at 8.3 eV below E_V was chosen as a reference. In case of a NEA surface, the sharp low energy peak corresponding to E_C can be used to find E_V, too. Then the difference between E_C and E_V corresponds to $h\nu - E_G$.

C. Results and Discussion

First, consider the diamond surfaces before metal deposition. After loading the samples into the vacuum system, AES scans were obtained. Features indicative of the presence of oxygen on the surface were detected. Subsequent to a 500°C anneal, the oxygen peak was only

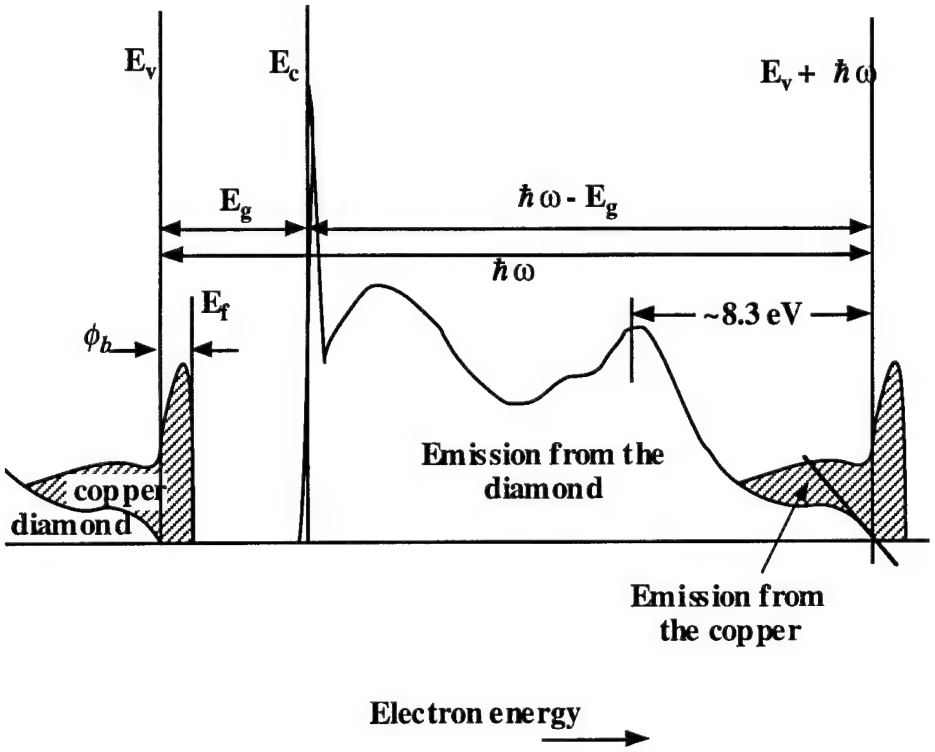

Figure 2. Schematic diagram of photoemission spectra for a metal (e. g. copper) deposited on diamond. The Schottky barrier height Φ_B is determined from the difference between the position of the valence band edge of diamond E_V and the metal Fermi level E_F.

slightly reduced. After a 1150°C anneal, oxygen was no longer observed by means of AES. From UPS spectra positive electron affinities of $\chi = 1.4$ eV and of $\chi = 0.7$ eV were found for the substrates heated to 500°C and 1150°C, respectively. These numbers were consistent with values reported previously [5, 9]. It is expected that chemisorbed oxygen on diamond results in a stronger surface dipole than for the clean surface. This would also lead to a larger workfunction for the oxygen terminated surface. Our observations are in agreement.

Following deposition of 2Å of Zr on clean diamond surfaces, the width of the UPS spectrum increased consistently with the surface exhibiting a NEA (Fig. 3a). A Schottky barrier height of $\Phi_B = 0.70$ eV was measured. Emission below the conduction band minimum E_C was observed. This phenomenon will be discussed further in another publication [16]. Deposition of 2Å of Zr on oxygen terminated diamond surfaces also resulted in a NEA. A larger Schottky barrier height of $\Phi_B \cong 0.9$ eV was measured (Fig. 3b). And the spectrum shifted ~ 0.3 eV toward lower energies. Subsequent to depositing 2Å of Cu on clean diamond surfaces a NEA and a Schottky barrier height of $\Phi_B = 0.70$ eV were determined by means of UPS (Fig. 4a). Also, the spectra shifted by 0.3 eV to lower energies. However, in the case of Cu on oxygen terminated surfaces, a positive electron affinity of $\chi = 0.75$ eV and a larger Schottky barrier height of $\Phi_B \cong 1.60$ eV were measured (Fig. 4b). Also, a larger shift to lower energies of 0.6 eV was found. These results are summarized in Table I. Equation (1) is valid

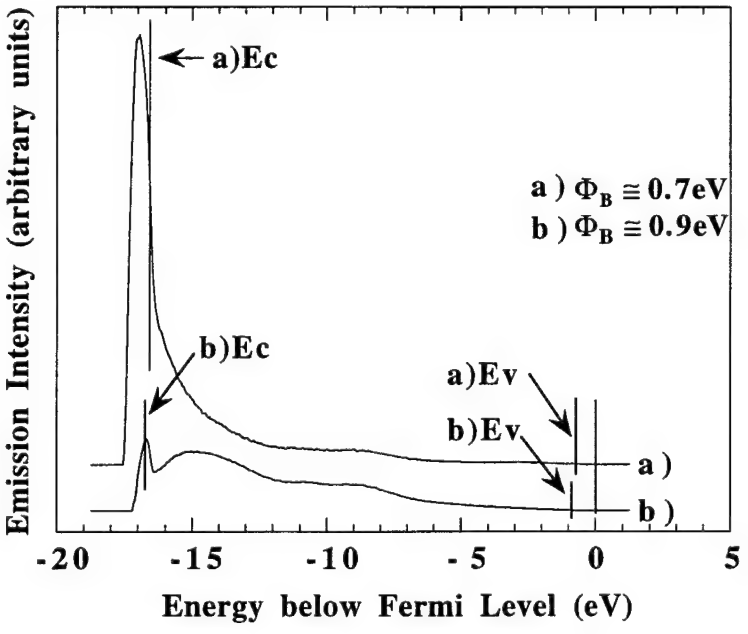

Figure 3. UV photoemission spectra of 2Å of Zr deposited on a diamond (100) surface annealed to a) 1150°C b) 500°C. Metal induced NEA's are observed upon deposition of Zr for both a) and b). For a) emission below E_C is detected.

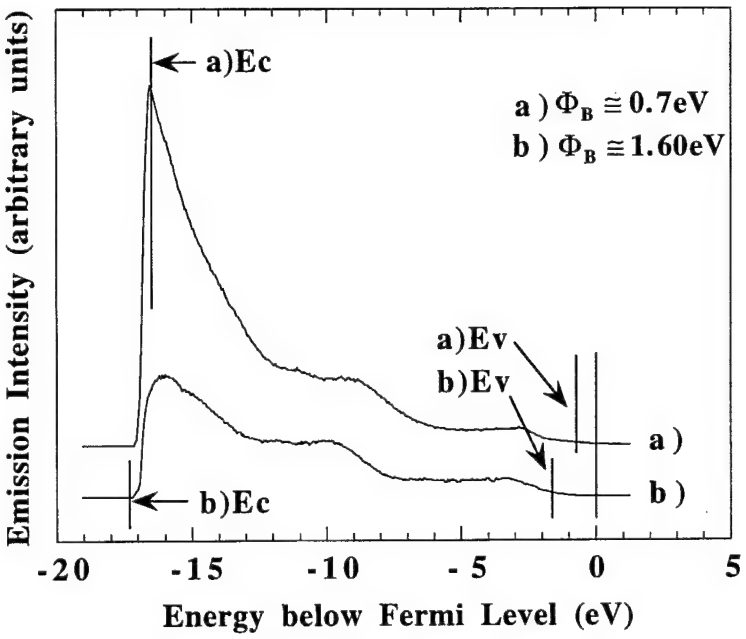

Figure 4. UV photoemission spectra of 2Å of Cu grown on a diamond (100) surface following an anneal to a) 1150°C b) 500°C. A metal induced NEA is observed for a) whereas a positive electron affinity is detected for b).

Table I. Results of UV Photoelectron Emission Spectroscopy to Measure Electron Affinity χ and Schottky Barrier Φ_B.

Sample	UPS Oxygen	Clean
C(100)	PEA, $\chi \cong 1.40$ eV	PEA, $\chi \cong 0.70$ eV
Zr/C(100)	NEA, $\chi < 0$, $\Phi_B \cong 0.90$ eV	NEA, $\chi < 0$, $\Phi_B \cong 0.70$ eV
Cu/C(100)	PEA, $\chi \cong 0.75$ eV, $\Phi_B \cong 1.60$ eV	NEA, $\chi < 0$, $\Phi_B \cong 0.70$ eV

PEA: positive electron affinity, NEA: negative electron affinity

specifically for photoemission of thin metal layers (less than the electron mean free path) on semiconductors: the electron affinity can be expressed in terms of the Schottky barrier formed with a p-type semiconductor [17].

$$\chi = (\Phi_M + \Phi_B) - E_G \quad (1)$$

Using the bandgap of diamond $E_G = 5.47$ eV, the workfunction of Zr ($\Phi_M = 4.05$ eV) and Cu ($\Phi_M = 4.59$ eV) and the measured Schottky barrier heights Φ_B, the electron affinities

can be calculated. For Zr, we obtain χ = - 0.72 eV for the clean surface and χ = - 0.52 eV for the oxygen terminated surface. In the same way, χ = - 0.18 eV and χ = 0.72 eV are obtained for Cu on the clean and oxygenated surfaces, respectively. These results are consistent with the NEA and positive electron affinity effects that were observed by employing of UPS. Figures 5 and 6 show energy band diagrams of the Zr-diamond and the Cu-diamond interfaces. These schematics illustrate the correlation of the Schottky barrier height with the electron affinity.

This simple workfunction model has been used successfully to explain NEA or positive electron affinity effects for systems like Ti or Ni layers on diamond (111) surfaces [7, 8]. It

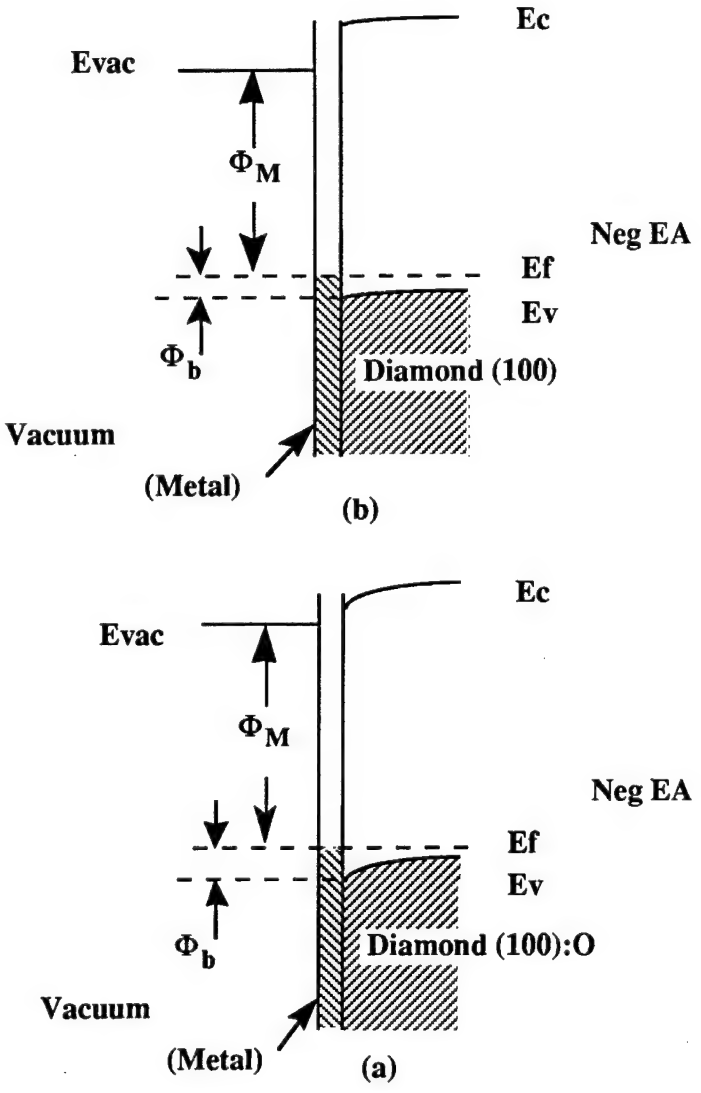

Figure 5. Band diagrams of the zirconium-diamond interface. For zirconium on both the oxygen terminated (a) and the clean surface (b) the Schottky barrier height added to the metal work function is less than the diamond bandgap. This corresponds to a NEA.

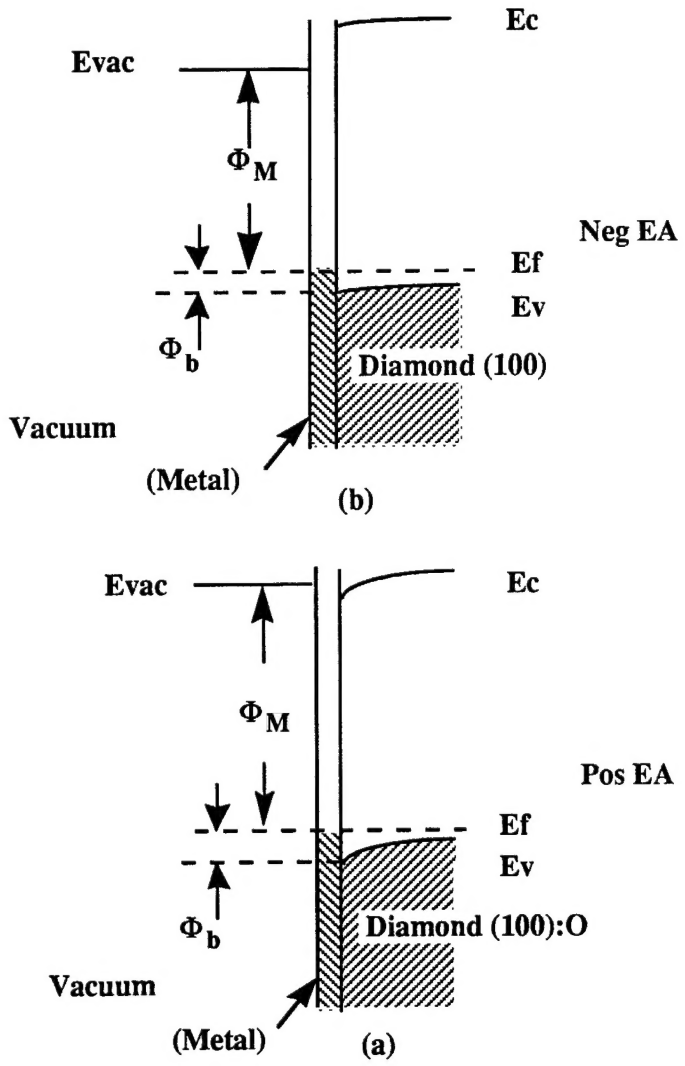

Figure 6. Band diagrams of the copper-diamond or cobalt-diamond interface. For copper or cobalt on the oxygen terminated surface (a) the sum of the Schottky barrier height and work function for metal on diamond is greater than the band gap of diamond resulting in a positive electron affinity. For copper or cobalt on the clean surface (b) the Schottky barrier height added to the metal work function is less than the diamond bandgap. This corresponds to a NEA.

has been found that Ni deposited on Ar plasma cleaned diamond (111) substrates induces a NEA. An Ar plasma or a 950°C anneal results in a (111) surface free of adsorbates [4]. In comparison, a larger Schottky barrier and a positive electron affinity were measured for thin Ni films on hydrogen terminated (111) surfaces. In theoretical studies by Erwin and Pickett [19-22] and Pickett, Pederson and Erwin [23] it was reported that the most stable configuration for Ni on clean (111) and (100) surfaces resulted in a Schottky barrier height of less than 0.1 eV. Considering copper on diamond (111) surfaces, Lambrecht [24] calculated a value for the Schottky barrier height of less than 0.1 eV for clean surfaces and greater than 1.0 eV for

hydrogen terminated surfaces. According to these results the interface termination appears to be have a significant effect on the Schottky barrier height. For metals deposited on clean surfaces, lower values for the Schottky barrier height and a greater likelihood of inducing a NEA are expected than for metals on non adsorbate free surfaces. The Schottky barrier heights reported in our study for Zr and Cu on diamond were consistent with this finding.

Apparently the Schottky barrier height for Zr on diamond does not depend on the surface termination of the diamond substrate as strongly as is the case for Cu. Both Zr on clean, as well as oxygen terminated diamond surfaces, tend to exhibit lower electron affinities than Cu on corresponding surfaces. This could be due to the higher reactivity of Zr with both C and O than Cu. It has been reported that Ti, as well as titanium oxide on diamond, exhibit a NEA [25]. Zr is next to Ti in the periodic table of elements and has properties similar to Ti. In our experiments, Zr could have reacted with the oxygen from the oxygen terminated surface. This may be indicative that Zr, as well as zirconium oxide on diamond, could exhibit a NEA. Zr, like Ti, does react with C. But this reaction is not expected to occur at room temperature. Ti was annealed to > 400°C before reaction with C was observed [26]. Cu on the other hand does not react as readily with C or O. Thus, the Cu-diamond interface structure for Cu on the clean diamond surfaces is different than for Cu on the oxygen terminated surfaces.

D. Conclusions

The effects of depositing thin metal films onto clean and oxygen terminated diamond (100) substrates has been studied by UPS. It was found that Cu induced a NEA on clean surfaces but not on oxygen terminated surfaces. In comparison, Zr induced a NEA on both clean and oxygen terminated surfaces. The Schottky Barrier height of Zr on diamond was less dependent on the termination of the diamond surface than was the case for Cu. This is attributed to the fact that Zr exhibits a strong affinity to the oxygen of the oxygen terminated diamond surfaces. In comparison Cu does not exhibit a significant tendency to form oxides.

E. References

1. F. J. Himpsel, D. E. Eastman, P. Heimann and J. F. van der Veen, Phys Rev. B **24**, 7270 (1981).
2. B. B. Pate, M. H. Hecht, C. Binns, I. Lindau and W. E. Spicer, J. Vac. Sci. Technol. **21**, 364 (1982).
3. P. K. Baumann, T. P. Humphreys and R. J. Nemanich, in *Diamond, SiC and Nitride Wide Bandgap Semiconductors*, edited by C. H. Carter, G. Gildenblat, S. Nakamura, R. J. Nemanich, (Mater. Res. Soc. Proc. **339**, Pittsburgh, PA, 1994), pp. 69-74.
4. J. van der Weide and R. J. Nemanich, Appl. Phys. Lett. **62**, 1878 (1993).
5. J. van der Weide, Z. Zhang, P. K. Baumann, M. G. Wensell, J. Bernholc and R. J. Nemanich, Phys. Rev. B **50**, 5803 (1994).
6. P. K. Baumann and R. J. Nemanich, *Proc. Diamond Films '94 of the 5th European Conference on Diamond, Diamond-like and Related Materials*, Eds. P. K. Bachmann, I. M. Buckley-Golder, J. T. Glass, M. Kamo: J. Diamond Rel. Mat. **4**, 802 (1995).

7. J. van der Weide and R. J. Nemanich, J. Vac. Sci. Technol. B **10**, 1940 (1992).
8. J. van der Weide and R.J. Nemanich, Phys. Rev. B, **49**, 13629 (1994).
9. P.K. Baumann and R.J. Nemanich, Appl. Surf. Sci. **104/105**, 267 (1996).
10. P.K. Baumann and R.J. Nemanich, in *Diamond for Electronic Applications*, edited by C. Beetz, A. Collins, K. Das, D. Dreifus, T. Humphreys, P. Pehrsson, (Mater. Res. Symp. Soc. Proc. **416**, Pittsburgh, PA, 1996), pp. 157.
11. P. K. Baumann, S. P. Bozeman, B. L. Ward and R. J. Nemanich in III-Nitride, SiC, and Diamond Materials for Electronic Devices, edited by C. Brandt, D. K. Gaskill, R. J. Nemanich, (Mater. Res. Soc. Proc. **423**, Pittsburgh, PA, 1996), pp. 143.
12. P. K. Baumann, S. P. Bozeman, B. L. Ward and R. J. Nemanich, *Proc. of Diamond '96, the 7th European Conf. on Diamond, Diamond-like and Related Materials jointly with ICNDST-5*, the 5th International Conf. on the New Diamond Science and Technology, edited by J. C. Angus, P. K. Bachmann, I. M. Buckley-Golder, O. Fukunaga, J. T. Glass, M. Kamo: accepted for publication in J. Diamond Rel. Mat. (1997).
13. F. J. Himpsel, P. Heimann and D. E. Eastman, Sol. State Commun. **36**, 631 (1980).
14. B. B. Pate, W. E. Spicer, T. Ohta and I. Lindau, J. Vac. Sci. Technol. **17**, 1087 (1980).
15. M. Marchywka, P. E. Pehrsson, S. C. Binari and D. Moses, J. Electrochem. Soc. **140** (2), L19 (1993).
16. P. K. Baumann and R. J. Nemanich, to be published (1997).
17. E. H. Rhoderick and R. H. Williams, *Metal-Semiconductor Contacts*, Clarendon, Oxford, (1988).
18. C. Weiser, Surf. Sci. **20**, 143 (1970).
19. S. C. Erwin and W. E. Pickett, Surf. Coat. Technol. **47**, 487 (1991).
20. S. C. Erwin and W. E. Pickett, Solid State Commun. **81**, 891 (1992).
21. W. E. Pickett and S. C. Erwin, Phys. Rev. B **41**, 9756 (1990).
22. W. E. Pickett and S. C. Erwin, Superlatt. Microsruct. **7**, 335 (1990).
23. W. E. Pickett, M. R. Pederson and S. C. Erwin, Mater. Sci. Eng. B **14**, 87 (1992).
24. W. R. L. Lambrecht, Physica B **185**, 512 (1993).
25. C. Bandis, D. Haggerty and B. B. Pate, in *Diamond, SiC and Nitride Wide Bandgap Semiconductors*, edited by C. H. Carter, G. Gildenblat, S. Nakamura, R. J. Nemanich, (Mater. Res. Soc. Proc. **339**, Pittsburgh, PA, 1994), p. 75.
26. J. van der Weide and R. J. Nemanich, *Proceedings of the First International Conference on the Applications of Diamond Films and Related Materials*, edited by Y. Tzeng, M. Yoshikawa, M. Murakawa and A. Feldman (Elsevier, New York, 1991), p. 359.

IV. Distribution List

Dr. Colin Wood Office of Naval Research Electronics Division, Code: 312 Ballston Tower One 800 N. Quincy Street Arlington, VA 22217-5660	3
Administrative Contracting Officer Office of Naval Research Regional Office Atlanta 101 Marietta Tower, Suite 2805 101 Marietta Street Atlanta, GA 30323-0008	1
Director, Naval Research Laboratory ATTN: Code 2627 Washington, DC 20375	1
Defense Technical Information Center 8725 John J. Kingman Road, Suite 0944 Ft. Belvoir, VA 22060-6218	2